Probing low temperature glass dynamics by fast generation and detection of optical holes

K.A. Littau [1] and M.D. Fayer
Department of Chemistry, Stanford University, Stanford, CA 94305, USA

Received 13 August 1990; in final form 7 November 1990

High resolution, fast optical hole burning results are reported for the amorphous system cresyl violet in ethanol glass at 1.3 K. Holes are burned and detected using a novel technique which allows precise detection of narrow ($\approx 0.03\ cm^{-1}$), shallow ($\approx 1\%$) holes 10 μs to 50 ms after their generation. The hole width is observed to change linearly when plotted against log time. Using a four point correlation model of optical hole burning, this spectral diffusion is shown to arise from a $1/R$ distribution of fluctuation rates. The distribution extrapolates to the value of the two pulse photon echo linewidth measured on the same system.

1. Introduction

Reported here are the results of waiting-time-(T_w)-dependent hole burning experiments on the system cresyl violet in glassy ethanol-*d*. The waiting time dependence, that is, the dependence of the hole linewidth on the waiting time between burning and detecting the hole, of cresyl violet in ethanol has been reported earlier in the range $0.1 < T_w < 4000$ s [1]. Using a novel technique described in section 2, this type of study is extended for the first time into the range 10 μs $< T_w < 0.1$ s. This combination of T_w-dependent data, which span many orders of magnitude in time, along with recent theoretical advances in analyzing waiting-time-dependent results [2] gives new information about the nature of the dynamics of low temperature glasses.

The dynamics of glasses and supercooled liquids, as well as other complex systems, are usually characterized by a very broad distribution of relaxation times. Thermodynamic properties and other phenomena are often observed to vary over decades of time [3]. Although this behavior is most often observed in the region of the glass transition temperature, several researchers [4–6] indirectly observed this phenomenon in the low temperature regime (< 1 K) with the discovery and subsequent modeling of non-Debye specific heats of inorganic glasses. The excess specific heat (relative to crystals) was attributed to low energy degrees of freedom, the so-called two level systems (TLS), which have both broad distributions of energies and relaxation rates (tunneling parameters). A TLS is described by an asymmetric double well potential with an energy asymmetry, E, and a tunneling parameter between the wells, λ. In the original TLS model the distributions of energies and tunneling parameters were assumed to be constant. This was sufficient to model the limited thermodynamic data available at that time. However, more realistic, system-dependent distribution functions are required to successfully model the vast amount of data now available. The TLS model along with these distribution functions is presently the best description of low temperature dynamics [1,7,8].

Since its use in describing anomalous heat capacity data, the TLS model has been used to successfully model the results of many other experiments on low temperature glasses. The results of thermal conductivity measurements [5,9] were successfully modeled by a distribution of TLS energies. The observation of acoustic phenomena, such as phonon echoes [10] and ultrasonic attenuation [11–13], has also been explained by the TLS model. The consistent observation of much broader than lifetime limited

[1] Present address: AT&T Bell Laboratories, Murray Hill, NJ 07974, USA.

linewidths detected by hole burning [14,15] and fluorescence line narrowing spectroscopy [16] has long been attributed to the existence of TLS. The temperature dependences of these linewidths, like the temperature dependence of thermodynamic data such as heat capacity, has provided information about the energy levels (density of states) of low temperature glasses.

Optical experiments also have the capacity to examine the distribution of dynamic processes in glasses. However, it was not until 1984 that this was demonstrated when the linewidth of spectral holes in a low temperature glass was shown to be time dependent [17]. Soon thereafter, stimulated photon echo data provided a further example of time-dependent linewidths in an inorganic glass [18]. In each case the linewidth was observed to broaden logarithmically over time. Later, hole burning and two pulse photon echo results were compared showing that the linewidth changes a factor of 6 between the time scales of the two experiments – nanoseconds to hundreds of seconds [19,20]. Since those reports, other systems have exhibited similarly dramatic time dependences [21–23].

Recent theoretical work of Bai and Fayer [2] permits the analysis of waiting-time-dependent experiments in a way which allows the underlying fluctuation rate distribution to be obtained. With this method, different waiting time experiments may be quantitatively compared since each may be used to calculate the fluctuation rate distribution. This type of analysis was recently reported for the system cresyl violet in ethanol glass [1]. Waiting-time-dependent hole burning data [1] and photon echo data [24] produced a preliminary outline of the fluctuation rate distribution which showed a $1/R$ distribution of the fast rates and a log normal distribution at much slower rates.

The motivation for the experiments reported here is to examine the intermediate rates, which traditional hole burning spectroscopy has not been able to access. The $1/R$ distribution of fluctuation rates obtained from the two pulse echo work on ethanol, glycerol, PMMA, and several other systems [19–21,25] has been shown to correspond to a flat distribution of tunneling parameters in the TLS model [20,26]. However, for ethanol, it has also been shown that this distribution must cut off before it reaches the hole burning time scale [20,21,26].

2. Theory of T_w-dependent optical dephasing

Recent work of Bai and Fayer [2] based upon the earlier work of several authors studying spin dynamics [27–29] and the four point correlation function description of optical observables [30] has produced a useful set of relations between the observables of waiting-time-dependent experiments and the underlying fluctuation rate distribution. This treatment has been given previously [1,2,20,26], and, therefore, only a brief description will be given here.

Time-dependent shifts in the resonant frequency of chromophores in a glass are responsible for time-dependent line broadening (spectral diffusion). In the TLS model these frequency perturbations are caused by interactions with the randomly fluctuating TLSs surrounding the chromophores. That is, the resonant frequency of a particular chromophore is dependent on the absolute states of the nearby TLSs. The term state refers to which side of the TLS asymmetric potential the TLS occupies. With time, the states of these TLSs will change due to phonon assisted tunneling. These fluctuations have a broad range of rates due to the distribution of TLS tunneling parameters. Thus, the resonant frequency of the chromophore will tend to drift. Therefore, if a sharp spectral feature such as a hole is prepared, it is only a matter of time before it is dulled due to interactions with the fluctuating environment. It is the four point dipole correlation function, which was mentioned above and is described elsewhere [2,30], which relates the fluctuations of the TLS to actual line broadening. By averaging the correlation function over all the internal parameters of the dye–glass system, one obtains a complete description of time-dependent linewidths.

The necessary averages of the correlation function have been carried out for the case of TLS-induced dephasing in glasses, and the resulting relationships between the rate distributions of TLS fluctuations and experimental observables such as hole linewidths have been calculated [1,2]. When the line shape is Lorentzian, it can be shown that the linewidth is given by

$$\Delta\omega_H(T_w) \propto \int dR\, P(R)[1-\exp(-RT_w)], \qquad (1)$$

where $P(R)$ is the fluctuation rate distribution which describes the density of fluctuating TLS as a function of their relaxation rate. Eq. (1) is the key to analyzing waiting-time-dependent hole broadening in terms of the fluctuation rate distribution. This relation will be used in section 4 to obtain $P(R)$ from the experimental data.

3. Experimental procedures

The sample studied was a 1.2×10^{-4} M solution of cresyl violet (Exciton) in ethanol-*d*. Previous work has found the hole width to be independent of concentration for these molarities [1]. It should be noted that the dynamics of ethanol-*d* are identical to those of ethanol [1,20,21]. Ethanol-*d* was chosen because it has factor of ≈ 20 lower *persistent* hole burning efficiency [20,21]. After placing in a 1 mm spectroscopic cuvette, the sample was quickly cooled to liquid helium temperatures in a ^{4}He bath cryostat. The cooling rate was rapid enough to avoid formation of the alternate glassy phase of ethanol which has been observed previously in thermodynamic and optical experiments [31,32].

All spectra were recorded on the red side of the 0–0 absorption at 620 nm. This is well to the red of the absorption maximum at 610 nm [24]. The optical density of the sample at this wavelength was 0.6. The laser source for this experiment was a Coherent model 559-21 scanning single-mode dye laser pumped by an Innova 90-5 argon ion laser run in all lines mode.

The basic concept of this experiment is similar to those reported previously in which waiting-time-dependent hole burning results were recorded in the range 0.1 to 5000 s [1,33]. A hole is prepared with a sufficiently short laser pulse and then is monitored over time. In the previous studies, hole spectra were recorded by subsequent scans of the dye laser [1], therefore data could not be obtained with waiting times any faster than ≈ 100 ms. To obtain data for shorter times, a new method was employed.

The method used is diagrammed in fig. 1. The single mode output of the dye laser was split into two

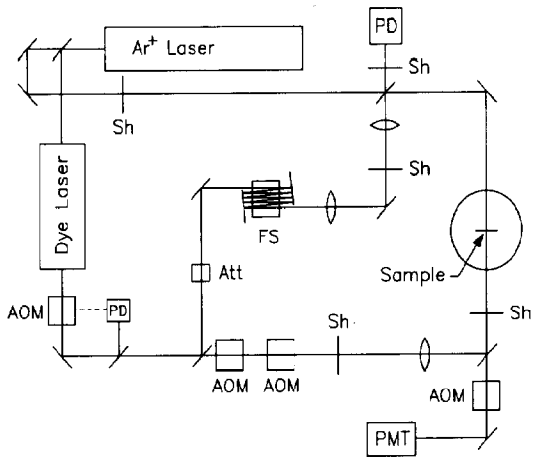

Fig. 1. Experimental apparatus used to record fast waiting-time-dependent optical holes. The dye laser output is split into burning and reading beams which run counterlinearly through the sample allowing continuous monitoring of the OD after burning. Sh – shutter; AOM – acousto-optic modulator; Att – variable attenuator; FS – frequency shifter, actually a multipassed 300 MHz AOM; PD – photodiode; PMT – photomultiplier tube.

beams. The first, dubbed the burning beam, was put through two 40 MHz acousto-optic modulators (AOMs) and a mechanical shutter before being focused onto the sample. The AOMs allowed an attenuation of $\approx 5\times10^5:1$ which could be switched in less than a microsecond and be controlled by computer. The shutter limited the AOM leakage exposure time to less than 1 ms. Two burning beam spot sizes were used – 150 and 450 μm.

The second beam, called the reading beam, passed through a variable attenuator, a frequency shifter, and a spatial filter before reaching the sample counter linear to the burning beam. The variable attenuator was a polarizer, $\frac{1}{2}\lambda$ plate, polarizer combination which had a dynamic range of $\approx 10^5:1$. The frequency shifter was a 250 MHz acousto-optic modulator driven at 300 MHz which was the upper limit of its bandwidth. The frequency of the reading beam could be shifted in steps of 300 MHz by successively sending the diffracted beam back through the modulator. Frequency shifts of up to 1.5 GHz could be accomplished in this fashion. Thus, instead of measuring the entire frequency spectrum at a single time, as has been done previously, the entire time dependence is measured at a single frequency. This is repeated for

a number of precisely controlled frequencies in 300 MHz steps.

The frequency shift was done at the expense of beam quality, however. Each pass through the frequency shifter distorted the beam profile. Therefore, the beam was passed through a spatial filter to clean it up before reaching the sample. Two reading beam spot sizes were used – 135 and 365 μm. All of the spot sizes used, both burning and reading, gave identical results. Table 1 is a list of burning and reading intensities used and the maximum depth of the transient holes obtained for each power.

After the sample, the reading beam was split off and sent into a cooled photomultiplier tube for detection. To protect the phototube from scattered light from the burning beam, which was typically 10^6 times more intense than the reading intensity, the beam was passed through an AOM which was switched off only during burning. Laser intensity fluctuations were controlled in two ways. An AOM controlled by a photodiode and feedback circuit (collectively called a "noise eater") stabilized the output of the laser. This controlled both short term noise and long term laser drift. A second photodiode monitored the laser intensity from a pickoff before the cryostat. This intensity was stored by computer and was later used to divide out laser intensity fluctuations not accounted for by the noise eater.

The burn/read sequence was as follows. Following a 100 ms read beam exposure to determine the baseline transmission, a 10–100 μs burn pulse generated a transient hole. The read beam transmission was then monitored for up to 100 ms. The data were collected by a 1 MHz, two channel, 12 bit ADC and stored. Following the acquisition of data, the computer corrected the data for laser intensity fluctuations and averaged it logarithmically (generating an equal number of time points per decade) reducing the data from 100 kbytes to 1 kbyte. In the time it took for the computer to average the data, the remainder of the transient hole had decayed leaving behind a negligibly small ($\approx$0.03%) persistent hole. Therefore data could be acquired repeatedly. Up to 100 shots were taken on the same spot. Smaller numbers of shots were taken on fresh spots yielding identical results.

When a small persistent hole had developed, the laser could be changed to a fresh spot or new frequency. However, to increase the rate of data acquisition, a hole erasing procedure was used. Laser-induced hole filling has been reported by a number of authors most notably Fearey, Carter and Small [34]. Irradiation of the sample at a frequency other than that which induced the hole will, under certain condition, reduce the hole area. To this end $\approx$250 mW of the argon ion laser beam was picked off before the data laser and used as a periodic erasing beam. With exposure times of $\approx$10 s, it erased essentially 100% of the hole without influencing the results of the waiting-time-dependent experiments. The data were identical whether the erasing procedure was used or new spots or frequencies were used. This will be discussed in detail subsequently [35].

Transmission versus waiting time data were recorded for each of six different shifted burning frequencies. Note that the data were not recorded simultaneously, but that each shifted frequency was recorded one at a time. When changing from one frequency to another, the reading beam direction shifted slightly, thus to ensure that good overlap between reading and burning beams was maintained, 200 μm (400 μm for larger spot sizes) pinholes on removable mounts were placed before and after the cryostat. By checking the transmission through the pinholes, the beams could be easily aligned. Small changes in alignment could be monitored in a simple

Table 1
Burn times and burn powers used to create spectral holes for cresyl violet in ethanol glass at 1.3 K

Spot size [a] (μm)	Burn time (μs)	Fluence (μJ/cm^2)	Transient hole depth [b] (%)	Reading beam intensity (μW/cm^2)
150	10	50	1.5%	15
450	100	100	2.2%	1.4

[a] Diameter of the intensity. [b] Maximum depth achieved.

way. Periodically during the acquisition of transient transmission data, a persistent hole was purposefully burned with the burning beam and scanned with the reading beam. The area of this persistent hole was proportional to the degree of overlap between the two beams in the sample. Thus small drifts or misalignments could be effectively normalized out. As a check of this procedure, after a transient transmission data set was collected, a second set was acquired with deliberately misaligned beams. Using the "normalization" holes, the difference between the data sets could be removed to within the signal to noise ratio limits.

To ensure that the pulsed burning conditions listed in table 1 were not artificially affecting the holewidths, persistent holes were burned by using a large number of pulses identical to those used to record the transient data. These holes were then scanned and the linewidths measured. Holes were burned both with pulsed conditions and with very low power (≈ 1 nW) cw beams and both before any erasing had occurred and after many holes had been burned and erased on the same spot. In each case, the holewidth was identical for identical waiting times (100 s) indicating that there was indeed no artificial hole broadening from burning with short pulses or from erasing. A detailed description of these tests will be published later [35].

Once a complete set of transmission versus waiting time data was acquired, it was converted to a set of 300 holes by taking time slices through the data. These holes were then fit by a least squares method to generate the holewidth versus time data reported in section 4. Several data sets were collected to ensure reproducibility. Once reproducibility was confirmed, the data sets were then averaged together.

4. Results and discussion

Fig. 2 shows change in optical density versus time curves for three of the six different read beam shift frequencies – 80 MHz, 680 MHz, and 1.28 GHz. The extra factor of 80 MHz is introduced by the two 40 MHz AOMs which modulate the burning beam. The solid lines through the data are best fits to a triple-exponential decay combined with a hole broadening function. The fits were not used to calculate the holewidth versus time data presented below. The raw

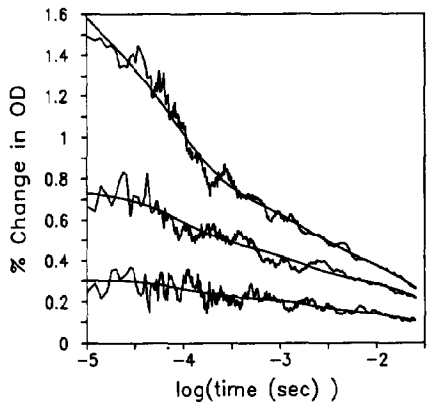

Fig. 2. Transient ΔOD plots for three different shifted reading beam frequencies for the system cresyl violet in glassy ethanol-*d* at 1.3 K. Shift frequencies relative to burning beam: top +80 MHz, middle +680 MHz, and bottom +1.28 GHz. The data is fit to a triple exponential decay as is described in the text.

data was used instead. The time scale studied in this measurement is in the range of the triplet lifetime of typical laser dyes. At low temperature, where spin-lattice relaxation is slow, three unequal triplet lifetimes are often observed [36]. The fact that the data may be fit to a triple exponential is consistent with, but does not prove, the notion that the transient holes observed here are caused by a triplet bottleneck with three different lifetimes. The best fit lifetimes are 60 ms, 1.5 ms, and 80 μs with magnitudes roughly in the ratio 5:2:4. There is no a priori reason to expect hole filling to be accompanied by hole broadening, and, indeed, earlier work performed at longer times suggests that there is no such correlation [1].

Fig. 3 shows two holes obtained at waiting times of 10 and 100 μs. Note that data are obtained for positive frequency shifts only. The data are reproduced on the negative side for display purposes. Fig. 4 is a full plot of the holewidth versus log waiting time. As can be seen in the figure, the holewidth shows a linear dependence on log time for waiting times faster than 100 ms. This yields a $1/R$ fluctuation rate distribution [26]. No deviation is seen from this distribution even at the fastest times.

Fig. 5a is a plot of the data of fig. 4 graphed along with the results of waiting-time-dependent holewidth studies obtained previously for $0.1 < T_w <$ 5000 s. The solid line is a fit of the combined data according to eq. (1), using a $P(R)$ which is log nor-

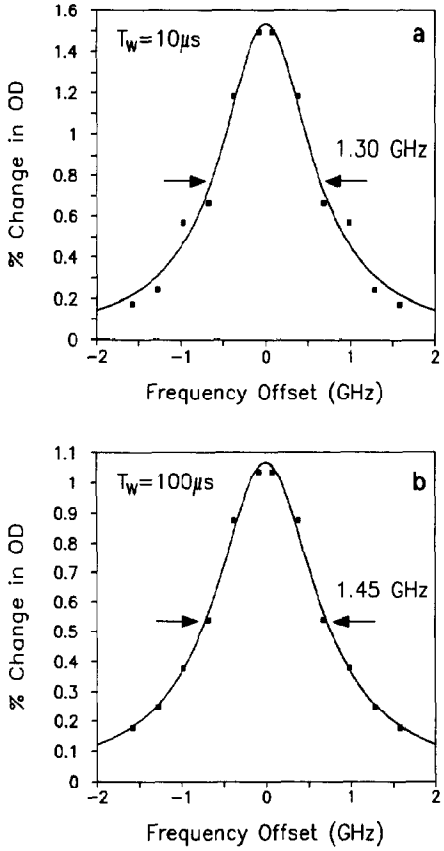

Fig. 3. (a) and (b): Two holes burned in the system cresyl violet in ethanol-*d* glass at 1.3 K and recorded with different waiting times. The solid lines are the best fit Lorentzians to the data.

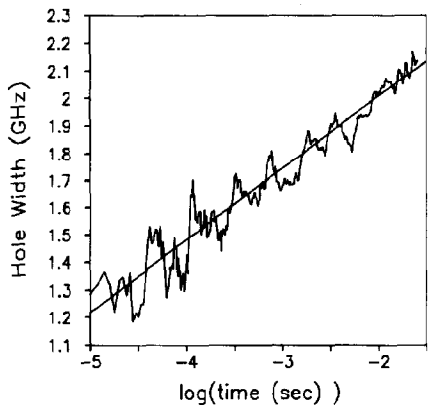

Fig. 4. Plot of holewidth versus log time in seconds for cresyl violet in ethanol-*d* at 1.3 K. The fact that the data broaden linearly when plotted versus log time indicates that the fluctuation rate distribution is $1/R$ in this region. The solid line is the best fit according to eq. (3) using a $P(R)$ which is $1/R$.

mal in the region beyond 1 s [1], and is $1/R$ at faster times. A log normal distribution in the slower region was determined previously using longer waiting time data [1]; however, the addition of a second log normal distribution at fast times does not adequately fit the data of fig. 4. A uniform $1/R$ distribution is required instead. The form of $P(R)$ which best fits the data is plotted as $P(R)*R$ in fig. 5b. The explicit form is

$$P(R)=\Delta\omega_1(\pi^{1/2}R\sigma)^{-1}\exp[-(\ln R_0-\ln R)^2/\sigma^2] + \Delta\omega_2 H(R-R_1)/R\,. \qquad (2)$$

H is a step function such that $H(x>0)=1$, 0 otherwise. The parameters which give the best fit are $\Delta\omega_1=0.97$ GHz, $\Delta\omega_2=0.115$ GHz, $\ln R_0=-4.1$, $\ln R_1=1.3$, and $\sigma=3.3$. The $1/R$ distribution cuts off abruptly according to eq. (2) as is shown in fig. 5b. This is, of course, unphysical. However, a function which decays smoothly to zero in less than one decade in time would produce a nearly identical time-dependent linewidth according to eq. (1). Note that the small rise just at the slow end of the $1/R$ distribution is from the tail of the log normal distribution.

Phenomenological models of glass dynamics predict a $1/R$ form for the fluctuation rate distribution. This arises naturally if one assumes a constant distribution of tunneling parameters when using the TLS model. This form of the distribution has been determined from two pulse photon echo data for fast rates [20,21,24,37] and has also been used to describe other aspects of glass dynamics [5,6,14]. It has been shown [20,26] that for such a distribution the four point correlation function is

$$C(\tau, T_w, \tau)=\exp\{-\beta\tau[\theta+\ln(T_w/T_{PE})]\}\,, \qquad (3)$$

where θ is a dimensionless constant equal to 3.6 [26]. β is a constant which includes the density of TLS and the TLS/chromophore coupling strength. Using this relation it is possible to calculate the two pulse echo linewidth from the $P(R)$ distribution given by the T_w-dependent hole burning data. This analysis will be published in detail elsewhere [35]. Letting $P(R)=\Delta\omega/R$ the relation is

$$\Gamma_{PE}=\Delta\omega\theta/2+\Gamma_0\,. \qquad (4)$$

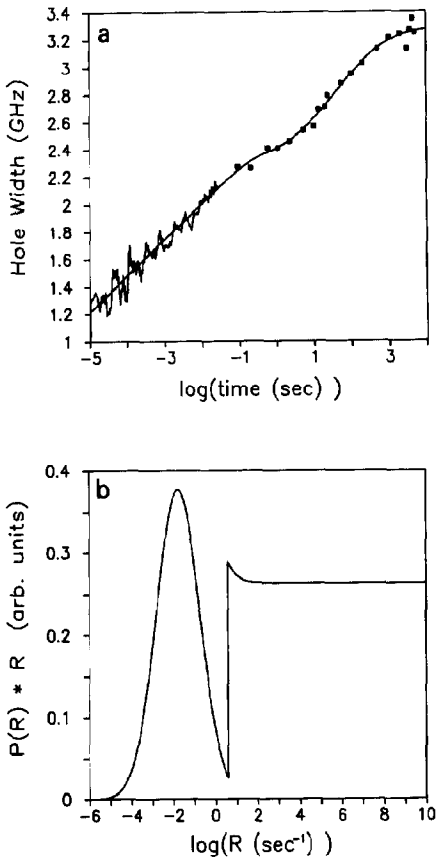

Fig. 5. (a) Plot of holewidth versus log time in seconds for cresyl violet in ethanol-*d* at 1.3 K. The data are plotted along with holewidth results obtained earlier (■) for the same sample and temperature [1]. Note that the new data fit smoothly into the data taken previously. (b) Plot of $P(R)*R$ versus log R used to fit the data in (a). $P(R)$ is $1/R$ at large rates and cuts off to a log normal distribution at slow rates. See text for values of the parameters. The small rise at the slow end of the $1/R$ distribution is from the tail of the log normal distribution. Extrapolating the $1/R$ distribution to the timescale of the two pulse echo gives good agreement with photon echo results (see text).

Where Γ_0 is the lifetime contribution to the linewidth. For cresyl violet in deuterated ethanol $\Gamma_0 = 28$ MHz [21]. Using the value of $\Delta\omega$ determined from the slope of the linear data of fig. 4 [35], i.e. $\Delta\omega = 0.115$ GHz, one obtains $\Gamma_{PE} = 230$ MHz for cresyl violet in ethanol-*d* glass at 1.3 K. Interpolating previously reported two pulse echo data gives $\Gamma_{PE} = 180$ MHz which is reasonable considering the scatter of the photon echo data [24]. However, since $P(R)$ is still undetermined in the four decades between 10 μs and 1 ns, it is possible that the echo interpolation is correct and that the value of $\Delta\omega$ at very large rates is somewhat smaller than what is observed from 10 μs to 50 ms.

These experimental results provide insight into the structure of the dynamics in low temperature glasses. Many previous experiments on glasses have focused on a single quantity, i.e. a linewidth or a heat capacity, measured at a single waiting time. Such experiments reduce the entire range of dynamics to a single point. However, the key to understanding the dynamics of glasses lies in understanding the entire dynamical spectrum. The fluctuation rate distribution for ethanol at low temperature is now known from 5000 s to 10 μs and from a few picoseconds to ≈ 1 ns. Experiments are currently in progress to fill in the remaining four decade gap in the distribution.

Acknowledgement

This work was supported by the National Science Foundation Division of Materials Research (No. DMR87-18959). Additional support was provided by the office of Naval Research, Physics Division (N000014-89-J1119). KAL would like to thank AT&T Bell Laboratories for a Graduate Fellowship.

References

[1] K.A. Littau, Y.S. Bai and M.D. Fayer, Chem. Phys. Letters 159 (1989) 1; J. Chem. Phys. 92 (1990) 4145.
[2] Y.S. Bai and M.D. Fayer, Phys. Rev. B 39 (1989) 11066.
[3] J. Wong and C.A. Angell, Glass structure by spectroscopy (Dekker, New York, 1976).
[4] R.C. Zeller and R.O. Pohl, Phys. Rev. B 4 (1971) 2029.
[5] P.W. Anderson, B.I. Halperin and C.M. Varma, Phil. Mag. 25 (1972) 1.
[6] W.A. Phillips, J. Low Temp. Phys. 7 (1972) 351.
[7] W.A. Phillips, ed., Amorphous solids: low temperature properties (Springer, Berlin, 1981).
[8] W.E. Moerner, ed., Persistent spectral hole burning: science and applications (Springer, Berlin, 1988).
[9] M.P. Zaitlin and A.C. Anderson, Phys. Rev. B 12 (1975) 4475.
[10] B. Golding and J.E. Graebner, Phys. Rev. Letters 37 (1976) 852.
[11] B. Golding, J.E. Graebner, B.I. Halperin and R.J. Schultz, Phys. Rev. Letters 30 (1973) 223.

[12] W. Arnold, S. Hunklinger, S. Stein and K. Dransfeld, J. Non-Cryst. Solids 14 (1974) 192.
[13] J. Jäckle, L. Piché, W. Arnold and S. Hunklinger, J. Non-Cryst. Solids 20 (1978) 365.
[14] J.M. Hayes, R. Jankowiak and G.J. Small, in: Persistent spectral hole burning: science and applications, ed. W.E. Moerner (Springer, Berlin, 1988).
[15] R. Jankowiak and G.J. Small, Science 237 (1987) 618.
[16] P.M. Selzer, D.L. Huber, D.S. Hamilton, W.M. Yen and M.J. Weber, Phys. Rev. Letters 36 (1976) 813.
[17] W. Breinl, J. Friedrich and D. Haarer, J. Chem. Phys. 81 (1984) 3915.
[18] M.M. Broer, B. Golding, W.H. Haemmerle, J.R. Simpson and D.L. Huber, Phys. Rev. B 33 (1986) 4160.
[19] C.A. Walsh, M. Berg, L.R. Narasimhan and M.D. Fayer, J. Chem. Phys. 86 (1987) 77;
M. Berg, C.A. Walsh, L.R. Narasimhan, K.A. Littau and M.D. Fayer, Chem. Phys. Letters 139 (1987) 66.
[20] M. Berg, C.A. Walsh, L.R. Narasimhan, K.A. Littau and M.D. Fayer, J. Chem. Phys. 88 (1988) 1564.
[21] D.W. Pack, L.R. Narasimhan and M.D. Fayer, J. Chem. Phys. 92 (1990) 4125.
[22] H. Fidder, S. de Boer and D.A. Wiersma, Chem. Phys. 139 (1989) 317.
[23] A. Rebane and D. Haarer, Opt. Commun. 70 (1989) 478.
[24] L.R. Narasimhan, D.W. Pack and M.D. Fayer, Chem. Phys. Letters 152 (1988) 287.
[25] A. Elshner, L.R. Narasimhan and M.D. Fayer, Chem. Phys. 128 (1989) 343.
[26] Y.S. Bai and M.D. Fayer, Chem. Phys. 128 (1988) 135; Comments Cond. Mat. Phys. 14 (1989) 343.
[27] P. Hu and S.R. Hartmann, Phys. Rev. B 9 (1974) 1.
[28] P. Hu and L.R. Walker, Phys. Rev. B 18 (1978) 1300.
[29] J.L. Black and B.I. Halperin, Phys. Rev. B 16 (1977) 2879.
[30] S. Mukamel and R.F. Loring, J. Opt. Soc. Am. B 3 (1986) 595;
S. Mukamel, Phys. Rev. A 28 (1983) 3480.
[31] O. Haida, H. Suga and S. Seki, J. Chem. Thermochem. 9 (1977) 1113.
[32] R. van den Berg and S. Völker, Chem. Phys. Letters 137 (1987) 201.
[33] Y.S. Bai, K.A. Littau and M.D. Fayer, Chem. Phys. Letters 162 (1989) 449.
[34] B.L. Fearey, T.P. Carter and G.J. Small, Chem. Phys. 101 (1986) 279.
[35] K.A. Littau, M.A. Dugan, S. Chen and M.D. Fayer, J. Chem. Phys., to be submitted.
[36] R. Avarmaa, Chem. Phys. Letters 46 (1977) 279.
[37] D.L. Huber, M.M. Broer and B. Golding, Phys. Rev. Letters 52 (1984) 2281.